SCIENTIFIC REPORTS

OPEN

Micro-Fresnel-Zone-Plate Array on Flexible Substrate for Large Field-of-View and Focus Scanning

Received: 20 July 2015
Accepted: 02 October 2015
Published: 30 October 2015

Mohammad J. Moghimi, Jayer Fernandes, Aditi Kanhere & Hongrui Jiang

Field of view and accommodative focus are two fundamental attributes of many imaging systems, ranging from human eyes to microscopes. Here, we present arrays of Fresnel zone plates fabricated on a flexible substrate, which allows for the adjustment of both the field of view and optical focus. Such zone plates function as compact and lightweight microlenses and are fabricated using silicon nanowires. Inspired by compound eyes in nature, these microlenses are designed to point along various angles in order to capture images, offering an exceptionally wide field of view. Moreover, by flexing the substrate, the lens position can be adjusted, thus achieving axial focus scanning. An array of microlenses on a flexible substrate was incorporated into an optical system to demonstrate high resolution imaging of objects located at different axial and angular positions. These silicon based microlenses could be integrated with electronics and have a wide range of potential applications, from medical imaging to surveillance.

The ability to implement microlens arrays on curved surfaces, inspired by natural compound eyes, provides unique optical properties[1–3]. In such a system, each individual microlens points in a different direction to capture an image of a specific part of a scene. Superposition of these images can then create an omnidirectional imaging system. Medical imaging, robot vision and surveillance cameras could all benefit from a large field of view (FOV) to maximize their observable extent[4,5]. Conventional microlens arrays are implemented on a planar rigid substrate which inherently limits their FOV. Arranging microlens arrays on curved surfaces can address this issue. Nonetheless, the curved surfaces are mostly fixed; therefore, the FOV and the depth of imaging are not reconfigurable. One approach to achieving a wide FOV while maintaining control of the imaging depth is to build microlens arrays on a flexible substrate so that they can be reconfigured into different forms in real time.

One of the main challenges in realizing fully functional optical systems (e.g. cameras) on flexible substrates is the integration of optics onto a soft layer[6,7]. Traditional fabrication techniques including photolithography, deposition and etching are mostly developed for planar rigid substrates[8,9]. Most organic materials and polymers are also not well suited for existing fabrication schemes[10]. For instance, high temperature, which most likely would be required in a deposition step, can significantly damage polymers. Additionally, integrating optical components onto flexible substrates while maintaining the quality of optical materials and structural accuracy is challenging.

In this article, we demonstrate an array of Fresnel zone plates (FZPs) as microlenses fabricated onto a flexible substrate. These microlenses were based on silicon and formed using silicon nanowires (SiNWs). Conventional semiconductor fabrication methods were utilized in a manner that circumvented existing challenges. The fabrication technique benefited from the ease of silicon (Si) processing while the polymer layer was not exposed to high temperature or destructive chemicals. The resulting near-perfect, black Si, comprised of SiNWs, was used to form binary FZPs with optimized focusing capability[11,12]. Fresnel imagers attract a great amount of interests due to their high angular resolution and large dynamic range[13,14]. They can also observe very distant objects and are functional over a large range of wavelengths, from

Department of Electrical and Computer Engineering, University of Wisconsin, Madison, WI USA. Correspondence and requests for materials should be addressed to H.J. (email: hongrui@engr.wisc.edu)

Lyman α to mid infrared[15]. Binary Fresnel lenses with alternating opaque and transparent zones are lightweight, compact and capable of providing high numerical apertures[16].

Since the FZP arrays were implemented on a deformable polymer substrate, the FOV is significantly increased compared to planar arrays[17,18]. The substrate bearing the FZPs can be bent so that each zone plate points at a different angle to capture images. We acquired images from individual microlenses simultaneously and stitched them together to produce a panoramic view of an object. Additionally, the flexibility of the substrate provided the opportunity to perform axial focus scanning by adjusting the position of the microlenses. The capability of high-resolution focus scanning was demonstrated by flexing the substrate so that the microlenses can capture images at various depths. This imaging system with microlens arrays on a flexible substrate can potentially provide images with a large FOV over a wide spectrum[19,20], resembling compound eyes[21]. Microlens arrays on polymer substrates could be utilized in contact lenses, laparoscopic surgery, displays and *in vivo* microscopy[22–30]. The fabrication of micro-FZPs based on Si nanostructures enables integration of microlenses with electronic circuitry on a monolithic platform.

Results

FOV and Focus Scanning of FZPs on Flexible Substrate. Figure 1 shows the schematic of our FZP microlens array. Each individual microlens is a FZP consisting of alternating opaque and bright zones. Unlike curved mirrors and refractive lenses, FZPs focus incident radiation into a spot via diffraction. In a FZP, radially symmetric rings modulate the phase of the incoming waves so that light rays from the bright zones constructively interfere to focus light. In order to minimize the reflectivity of the dark zones and to improve the focusing capability of the microlenses, black Si, made of a forest of SiNWs, is utilized to create near-perfect absorbing regions, with an absorption that is higher than 98% for the visible spectrum. The SiNWs are highly absorbent in the visible range owing to the nanoscale surface roughness and the low refractive index[31]. An aluminium (Al) layer, with a reflectivity of more than 90% on average in the visible range, is utilized for the bright zones to maximize reflection[32]; however, for transmissive lenses the Al is stripped off to achieve bright zones on the clear flexible substrate with a transmittance over 95%. The absorption of bright zones for both reflective and transmissive FZPs is significantly smaller compared to black Si. The high contrast between the absorption of the zones produces an efficient diffractive microlens. Figure 1a,b illustrate the transmissive micro-scale FZPs on a planar and curved substrate, respectively. The positions of the microlenses can be changed by the deformation of the flexible substrate as shown in Fig. 1b. Figure 1c shows the FOV of two lenses on a flat substrate with substantial overlap in their individual FOV. The flexibility of the substrate allows the microlenses to point at different angles and thus significantly increase the total FOV of the array from the planar arrangement, as shown in Fig. 1d.

Another advantage of building microlenses onto a flexible substrate is to achieve optical focus scanning, which allows for control over the imaging depth. Figure 1e,f show that axial focus scanning can be achieved by deformation of the flexible substrate. The focal length of the microlenses is fixed at f and is determined by the FZP geometry. However, the positioning of the microlenses depends on the shape of the substrate, and therefore the location of the focus can be shifted when the shape of the flexible substrate is reconfigured (Fig. 1e,f). The total range of the focus and speed of focus scanning depend on the size of the microlenses as well as on the mechanical properties of the substrate.

The focal length of each FZP can be calculated from diffraction theory. The radius of successive zones can be calculated from $r_m = \sqrt{m\lambda f + m^2\lambda^2/4}$, where λ is the wavelength of the incident waves and m is an integer number. The zones should switch from dark to bright at radius r_m. For a zone plate with a radius R, the field distribution at the first focus with a focal length of f approximately r_1^2/λ is described in Eq. 1

$$u(r, z = f) = 2\pi R^2 e^{i2\pi\frac{r^2}{\lambda f}} \frac{J_1(2\pi Rr/\lambda f)}{2\pi Rr/\lambda f} \quad (1)$$

where J_1 is the first Bessel function, z is the distance to the lens, and r is the radial coordinate in the first focal plane. Field distribution, and thus the intensity of the focused light, is independent of angle because the FZP is radially symmetric (see supplementary Fig. 1. and note 1, 2). The resolution of the FZP is 1.22 Δr based on Rayleigh criterion, where Δr is the thickness of the outermost ring (see supplementary Fig. 2).

Fabrication of FZPs on Flexible Substrate. The main steps for the fabrication process of a FZP microlens array on a flexible substrate are illustrated in Fig. 2. FZPs consisting of alternating dark and bright zones are first built on a rigid substrate using conventional semiconductor processes. A layer of Al with a thickness of 100 nm is sputtered and patterned on the polished side of a Si wafer using standard photolithography procedures. The Al layer serves as the bright zones as well as a hard mask for dry etching later. The dark zones are created on the rigid substrate between the Al rings. SiNWs are formed by etching the Si using a reactive-ion etch (RIE) process to achieve near-perfect black zones as illustrated in Fig. 2a. In order to create a flexible substrate to support the FZPs, a layer of polydimethylsiloxane

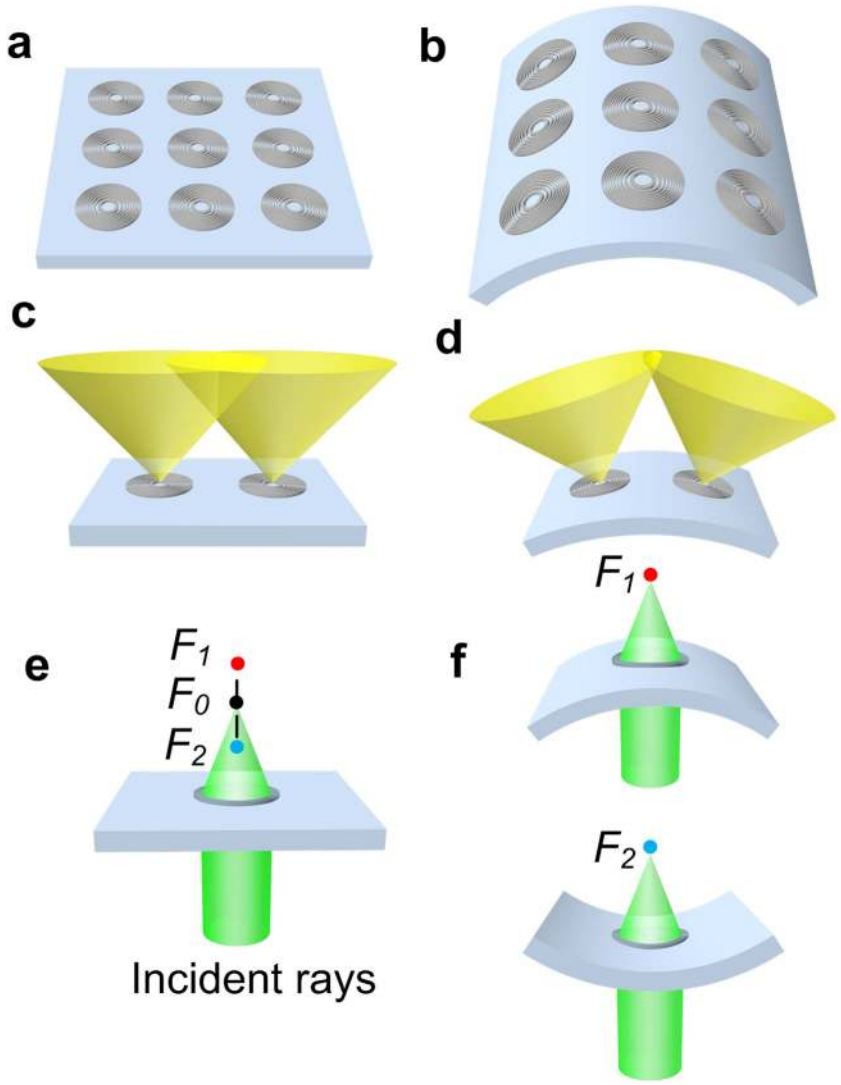

Figure 1. Schematic of FZPs. (**a**) An array of transmissive FZPs on a planar substrate. (**b**) FZPs on a flexible substrate with a convex shape. (**c**) The FOV for two FZPs on a flat substrate with substantial overlap. (**d**) The overall FOV is increased for the two FZPs on a flexible substrate due to the bending of the substrate. The FOV of a single FZP (microlens) is shown in yellow. (**e,f**) Focus scanning with a microlens on a flexible substrate. The focus when the substrate is flat is located at F_0. The focus shifts to F_1 for a convex shape of the substrate. The focus shifts to F_2 for a concave shape of the substrate. The total range of focus scanning is $\Delta F = F_2 - F_1$. Irradiance is shown in green. Reflective FZPs can also be realized, and their operating principle is similar to what is illustrated here.

(PDMS) prepolymer is spun, degassed and baked to create an elastomeric layer (PDMS) with enhanced mechanical properties on the surface of the Si wafer. At this stage, the FZPs comprising the nanowires and Al are sandwiched between the PDMS layer and the Si substrate as shown in Fig. 2b. As a final step, the rigid Si is etched away from the back side using Sulfur hexafluoride (SF_6) to release the PDMS. Thus, FZPs on a flexible substrate are achieved. The bulk etching of Si leaves the Al rings on the surface of the PDMS for bright zones and the embedded SiNWs inside the PDMS for dark zones. The final etching process is performed at room temperature so that PDMS is not exposed to high or low temperature. Throughout the fabrication procedures, the PDMS layer is not exposed to acids or bases. The process yield is very high, since this process eliminates the need to physically transfer the nanowires from the Si substrate to the PDMS layer (see supplementary Fig. 3).

Figure 3a shows a scanning electron microscope (SEM) image of an SiNW forest. The diameter of the wires varies from 20 nm at the tip to 400 nm at a depth of 1 μm. The length of the nanowires is roughly 2 μm. The morphology of the forest of nanowires results in the low reflectivity of black Si[31]. Figure 3b shows an SEM image of the nanowires embedded in a PDMS matrix. SiNWs are surrounded and supported by the cured polymer. Figure 3c shows an SEM image of a completed FZP microlens with

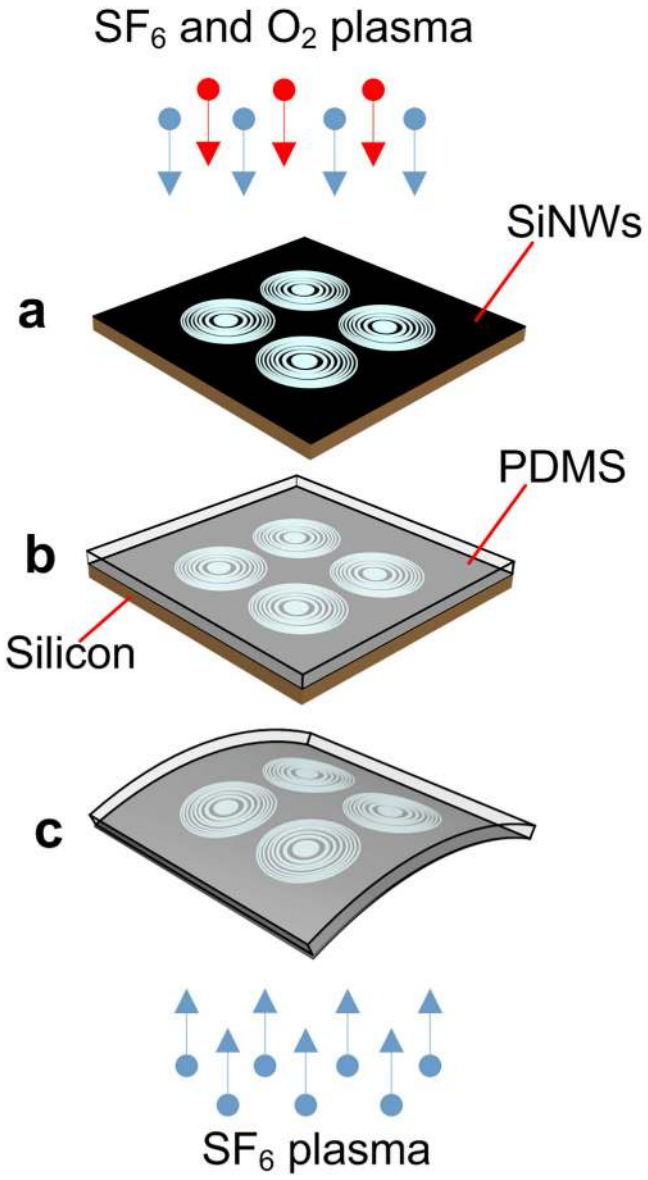

Figure 2. Main steps of fabrication process. The FZPs are fabricated onto a rigid and flexible substrate along with the SiNWs structure (**a**) 100 nm of highly reflective Al is deposited and patterned as rings on a Si substrate for bright zones. SiNWs are subsequently formed into the wafer surface by etching to create near-perfect absorbing (dark) zones between the Al rings using an RIE process with SF_6 and O_2 plasma. (**b**) Prepolymer of PDMS is spun on the wafer and then degassed to cover the SiNWs. The Al layer and the SiNWs are sandwiched between the PDMS and the Si wafer. The PDMS layer is then cured to create a flexible substrate. (**c**) Bulk etching at room temperature is performed on the back of the wafer to release the PDMS layer bearing the Al rings and the SiNWs. The processing gas is SF_6 for this bulk etching step. SiNWs are embedded into the PDMS matrix to achieve flexible FZPs.

a diameter of 400 μm and 15 zones. Figure 3d shows a microlens array under an optical microscope. The dark regions are evident between the Al rings. In addition, the black Si in between the FZPs creates integrated apertures for individual FZP microlenses. This aperture eliminates undesired stray reflections, which helps avoid double imaging and background haze. Two photographs of a micro-FZP array with 100 elements fabricated onto a PDMS layer are depicted in Fig. 3e,f. The array on the flexible PDMS substrate can be wrapped on many curved surfaces. As shown in the figure, the FZP microlens array can be curved, flexed and stretched.

Finite element analysis (FEA) was used to simulate the mechanical properties of the device and to examine the stress and strain experienced by the FZPs under deformation. The mechanical properties of the PDMS membrane are vital to the ability of the FZPs to adjust focus and offer wide FOVs. In order to simulate the device structure, we used devices with an overall diameter of 450 μm and a pitch size

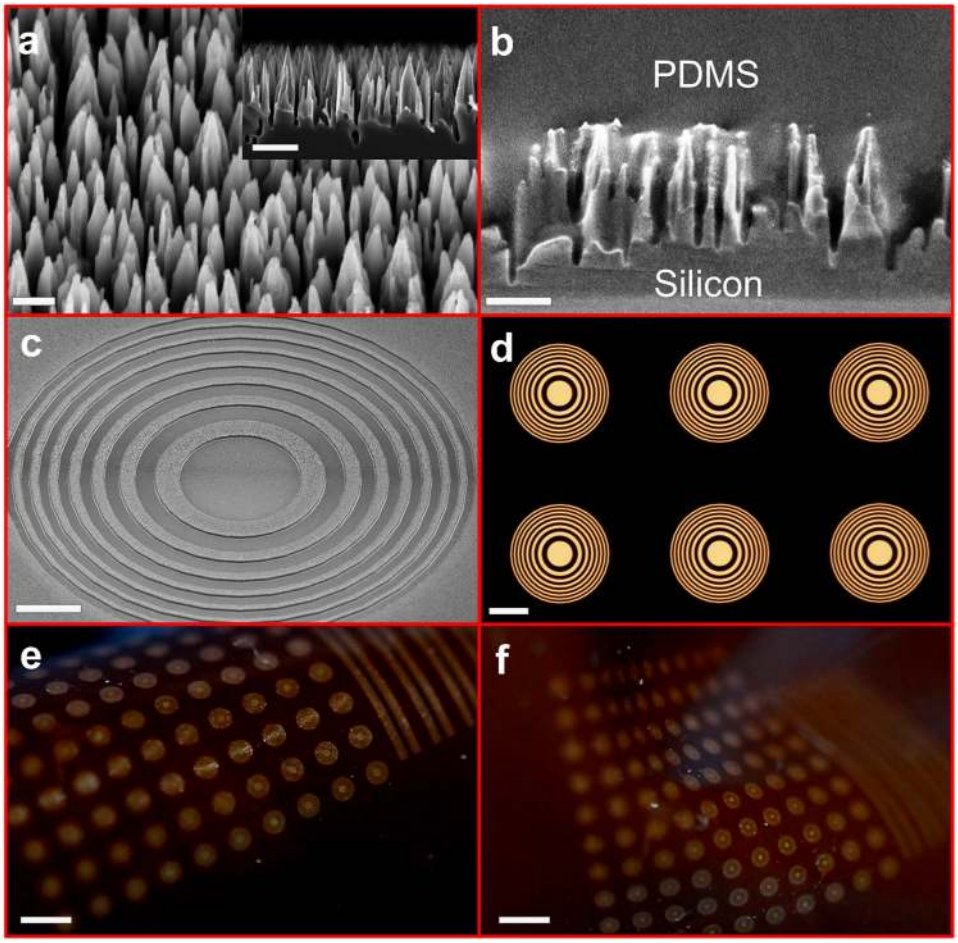

Figure 3. Completed devices. (**a**) SEM images of an SiNW forest for both cross sectional and tilted view at the angle of 45°, showing the tapered shape of the wires. The spacing between wires is 400 nm at the tips. Scale bar is 500 nm. Inset: cross-sectional view of silicon nanowires showing their tapered shape. Scale bar is 1 μm. (**b**) SEM of SiNWs embedded into PDMS matrix. (**c**) SEM of a single FZP with 15 zones. Scale bar is 40 μm. (**d**) An array of FZPs under an optical microscope: dark zones – SiNWs; bright zones – Al. The areas between FZPs are black Si which minimizes unwanted reflections. Scale bar is 400 μm. (**e**) Photograph of a completed array of FZPs on a flexible substrate. Scale bar is 1 mm. (**f**) The array of FZPs is flexed and stretched. Scale bar is 1 mm.

of 500 μm, representative values for our experimental devices. Figure 4a shows the total deformation of the device wrapped about a rod with a 1-cm diameter. The equivalent elastic strain solution is shown in Fig. 4b. It can be clearly seen that the FZPs experience insignificant strain with values of approximately 4×10^{-5} mm/mm for the central zone plates and 1×10^{-4} mm/mm for the outermost zone plate. The PDMS membrane in between the FZPs experiences the maximum amount of strain with values of approximately 1×10^{-3} mm/mm at the outermost edges and 3×10^{-4} mm/mm at the point of maximal curvature. This clearly indicates that the zone plates maintain their structural integrity during the process of deforming, bending and wrapping of the membrane, thus allowing for high-quality imaging and the ability to obtain a large FOV. We also looked at the change in the radius along both x and y directions of the FZP microlenses under extreme deformation. Both ends of the PDMS membrane were fixed while applying a force in the $+z$ direction in order to simulate the deformation. As observed in Fig. 4c, there is no significant change in the radius in both directions, until a deformation threshold of around 0.1 mm from the origin is reached, following which the deformation in the x and y directions show a non-linear increase. (see supplementary note 3 for more detail).

In addition, we simulated the mechanical properties of FZPs with SiNWs embedded in PDMS in order to examine the effect of FZPs on the flexibility of the substrate. While the elastic modulus of PDMS is around 500 kPa, the FZPs based on SiNWs have a value of 4 MPa. The underlying reason for an order of magnitude change can be attributed to the stiffness of SiNWs. Based on our simulations, the minimum achievable curvature is 14 mm. FZPs in this curvature still maintain their optical quality.

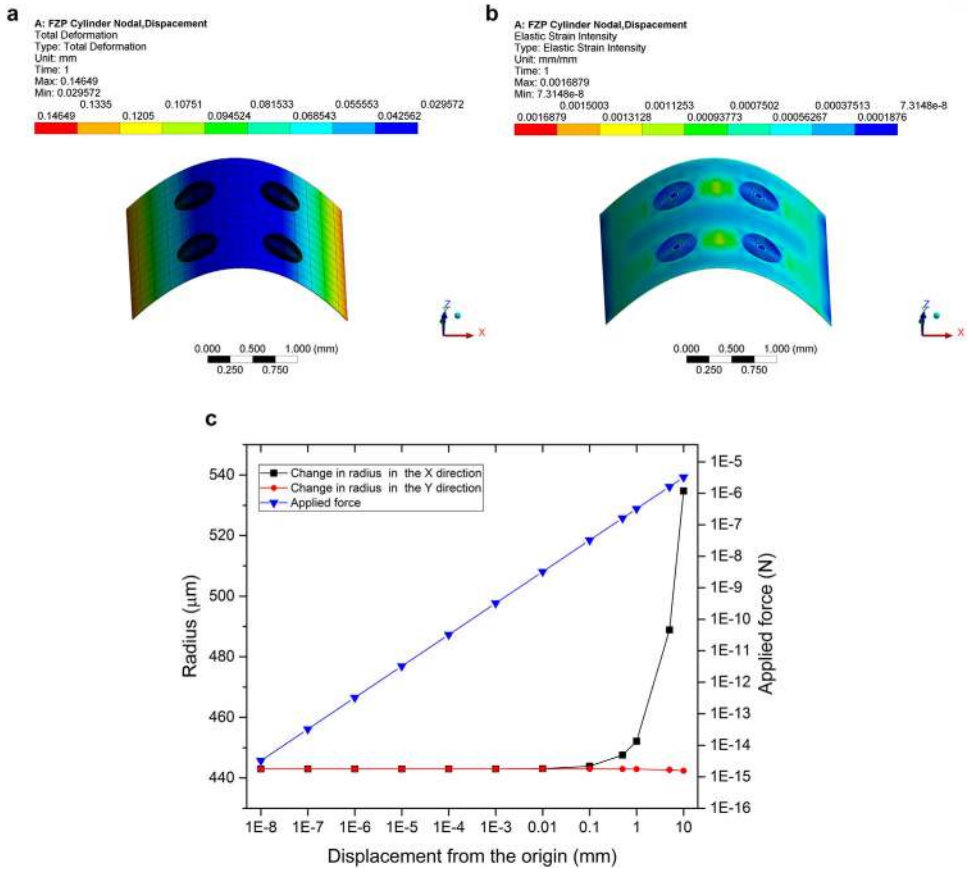

Figure 4. Mechanical Characterization of FZPs. FEA was utilized to determine the strain experienced by the FZP microlenses under deformation. (**a**) Total deformation of the device when wrapped about a cylindrical metal rod with a radius of 5 mm. (**b**) Elastic strain intensity solution of the device when wrapped about a cylindrical metal rod with a radius of 5 mm. The FZPs experience insignificant strain while most of the strain is seen in the deformable PDMS membrane. (**c**) Change in the radius of the FZPs in the x and y directions under deformation. The level of deformation is measured in terms of the displacement of the center of the membrane from the origin of the device. The amount of applied force is also measured and plotted.

High Resolution Imaging with FZPs on Flexible Substrate. The focusing ability of FZPs was characterized using an optical microscope (see Supplementary Fig. 4). The imaging capability of the FZP microlenses was demonstrated using an optical system to image an object as depicted in Fig. 5a. In this setup, an array of FZP microlenses on a flexible substrate is used in a high-resolution imaging system. The lens array is placed in front of a Nikon objective lens. A cubic beam splitter (BS) is used to separate backscattered light from the object and the beams reflected from the FZPs. The rays from the object reach the FZP array through the lenses and BS. Then, the rays reflected from the FZP passes through the BS and the camera lens to create an image on a CCD imager. The lens array was used to capture images from different parts of the object at various angles as shown in Fig. 5b. This capability can increase the extent of vision of a camera. As illustrated in Fig. 5, the total area imaged by the lens array is larger than the area covered by a single lens. A University of Wisconsin – Madison Bucky Badger head logo was used as the object. Nine microlenses, which are slightly curved with a radius of curvature of 10 cm, provided nine individual images of the logo. As illustrated in Fig. 5b, the images from the individual FZP microlenses were captured so as to ensure significant overlap between images from adjacent microlenses. The images from the microlens array were stitched together using the software PTGui^{TM}, to produce a complete image (Fig. 5c). The overlap between the images allowed them to be stitched with high fidelity. The stitching resulted in a 3.8 × increase in the area of the image captured by the lens array ($7 \times 7\,mm^2$) as compared to the area captured by a single lens ($12.56\,mm^2$). Both the horizontal and vertical extents of observation were increased by stitching the images from the microlens array. The total extent of vision covered by the array is approximately 1.75 times larger than that of a single lens. Although the array was slightly curved for this experiment, the FOV was increased from 14° for a single lens to 18° for a stitched image in Fig. 5c. More calculation regarding FOV, extent of observation and focus scanning are illustrated in Fig. 6. The overall FOV of two lenses on a flexible substrate with a bending angle β is

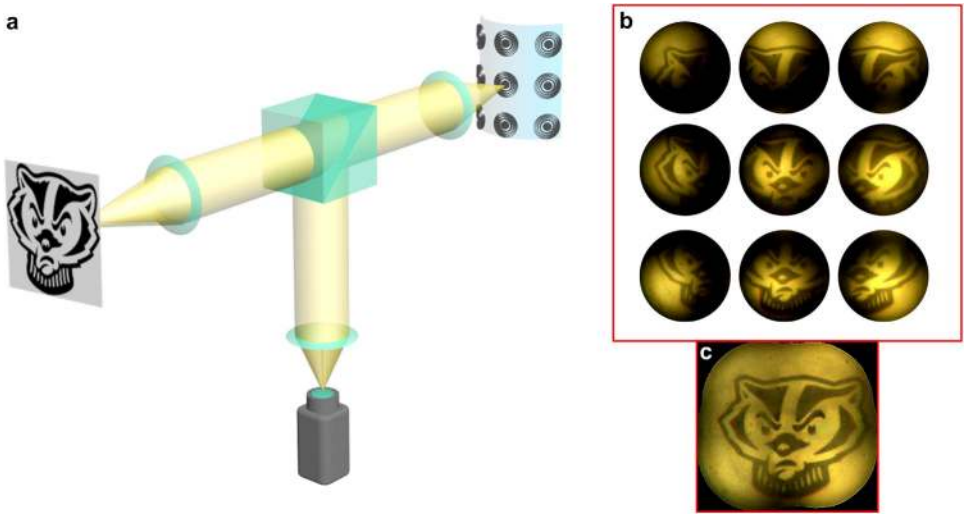

Figure 5. Imaging by a lens array. An array of FZP microlenses on a flexible substrate installed in a high resolution microscope. The lens array is placed in front of a lens of an assembled optical microscope. A beam splitter (BS) is used to separate the object beam and the beam reflected from the FZPs. The rays from the object reach the FZP array through lenses and BS. Then, the rays reflected from the FZP pass through the BS and the camera lens to create an image captured by a CCD camera. A University of Wisconsin – Madison Bucky Badger head logo printed on a transparency is used as the object (with permission from the University of Wisconsin – Madison). (**a**) Microlenses are pointing at different angles to capture images with a wide FOV. (**b**) Individual images acquired by nine lenses in a FZP microlens array. There is overlap between adjacent images from the individual lenses. (**c**) After stitching, the extent of view is significantly increased.

increased to $\alpha+\beta$ where α is the FOV of a single FZP (Fig. 6a–c). Figure 6d–f show that the location of the focus shifts to F_1 and F_2 when the substrate is flexed up and down.

Calculations show that FZPs on a flexible substrate can substantially increase the FOV. To demonstrate this, an array of FZPs was wrapped around a 1 cm-diameter cylindrical rod, so that each individual microlens pointed at a different angle as shown in Fig. 7. The overall angle of view of microlenses (diameter: 400 μm; pitch: 500 μm) was measured to be 170°, in which neighboring lenses maintained a slight overlap in the FOV. All the lenses across the 170° of combined FOV generated high-quality images.

Another attribute of the FZP microlenses on a flexible substrate is the ability to control the imaging depth. An artificial fly was used as an object. A FZP microlens on a flexible substrate was integrated with an imaging system as shown in Fig. 8a. The substrate was flexed with an external force to scan the focus of the microlens back and forth, by which process the imaging depth of the whole imaging system was changed (see Supplementary Movie 1). Figure 8 shows the focused images of different spatially separated features as the focus of the microlens was shifted. The resolution of the imaging system incorporating the FZP microlens was measured to be 8.8 μm (see Supplementary Fig. 5).

Discussion

In this article, a concept for wide FOV imaging along with focus scanning capability is introduced using FZP microlens arrays fabricated onto a flexible substrate. An array with 100 micro-scale FZPs was embedded into a PDMS layer as an elastic substrate. To achieve Si-based microlenses, the FZPs were created using black Si made of forests of SiNWs. The PDMS layer and all the devices within it were first built on a Si substrate; therefore, the fabrication technique is compatible with conventional Si processes. In addition, transferring the SiNW-based device structures to PDMS was performed by a standard bulk etching technique, which significantly improves the process yield. Such technique allows for fabrication of both transmissive and reflective FZPs for various applications.

The mechanical analysis of PDMS bearing FZPs indicated that the FZPs did not undergo significant strain when the PDMS substrate was deformed. Rather, most of the strain occurred in the PDMS, which maintained the image quality. The presence of SiNWs embedded in polymer increases the elastic modulus of the PDMS substrate by an order of magnitude (to about 4 MPa). Yet, the structure is still flexible to be bent to a minimum radius of curvature of 14 mm. The devices with such mechanical properties can potentially be curved into complex 3D structures such as a hemisphere.

The flexibility of the polymer substrate enables the FZP microlens array to have a large FOV for panoramic imaging. The exceptionally wide FOV may open up a viable path to an omnidirectional imaging system when combined with a flexible image sensor. In this work, we showed that the FOV of the micro FZPs can be increased to 170°. In our experiment, the number of FZPs as well as maximum FOV is

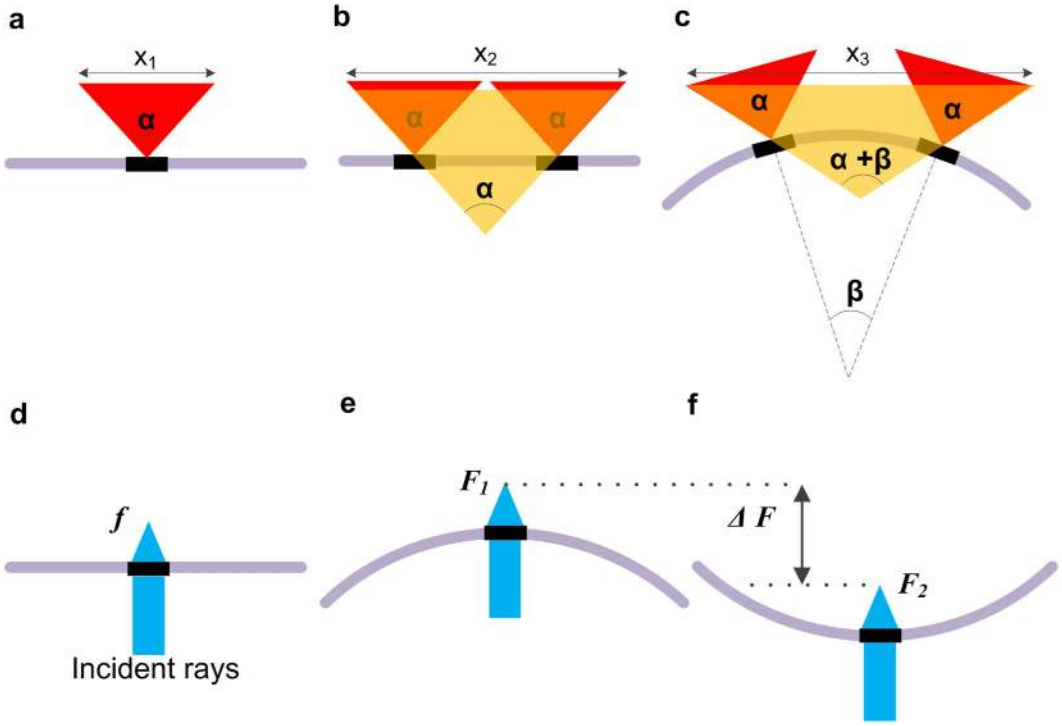

Figure 6. Wide FOV and Focus scanning concept. (**a**) The FOV of a single microlens is α and the extent of observation is X_1. (**b**) The FOV of two lenses on a rigid substrate is still α; however, the extent of observation X_2 is increased by the array. (**c**) The overall FOV of two lenses on a flexible substrate with bending angle β is increased to $\alpha+\beta$. The extent of observation at a fixed distance X_3 is significantly increased by the use of the lens array on a flexible substrate ($X_3 > X_2 > X_1$). (**d**) The focal length of a single microlens on a planar substrate is *f*. (**e,f**) The focus scanning can be achieved by flexing the microlens on a flexible substrate. The location of the focus shifts when the substrate is flexed. For all calculations, the area and the geometry of the sensor are considered fixed.

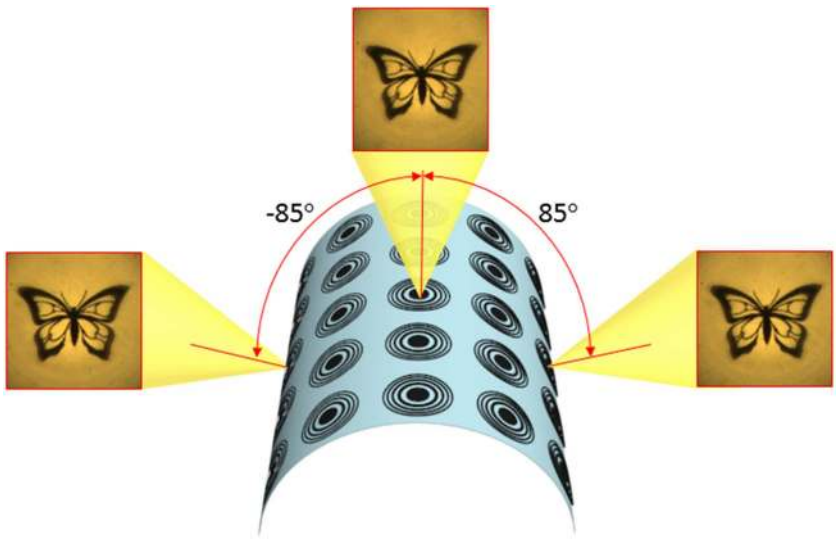

Figure 7. FOV of a microlens array on a curved shape. A wide angle of view is provided by microlenses distributed on a cylindrical surface. High-quality images of a printed butterfly (original butterfly image courtesy of FeaturePics.com/photo by xedos4) can be obtained across the FOV (shown at −85°, 0° and 85°). The overall FOV is 170°.

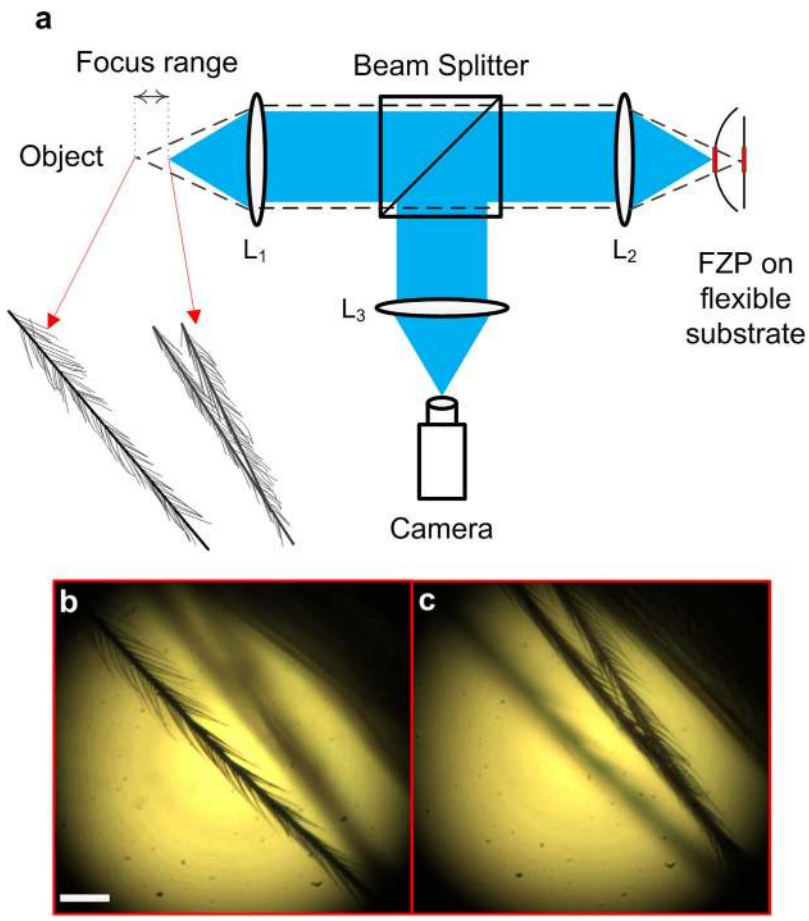

Figure 8. Focus scanning demonstration. A FZP on a flexible substrate is incorporated into a high-resolution imaging system to capture images of features of an artificial fly. Two parts of the hackle of the fly at various distances from the objective lens are imaged following the concept shown in Fig. 1f and Fig. 6f, where the substrate is flexed to scan the focus. (**a**) Deformation of the substrate changes the location of the microlenses so that the overall focus of the microscope is adjustable. The dashed rays and the solid rays distinguish how the rays hit the objects for the two different focal states. Schematic of two objects (hairs in the hackle of fly) located at two different positions is depicted in the figure. The distance between the objects is 500 μm. (**b**) The closer feather is in focus while the others are out of focus. (**c**) The further feathers are in focus while the closer one is out of focus. Scale bar is 500 μm.

limited by the parts in the optical setup available to us. However, combination of the FZPs on flexible substrate with flexible image sensor could maximize the FOV of the imaging systems to 360°.

Furthermore, the flexibility of the substrate allows the compact and lightweight FZPs to flex which results in axial scanning of the focus. This capability is particularly important in microscopy to acquire noninvasive, *in vivo* images of vital tissues at varied depths. The capability of the FZP microlens arrays to simultaneously increase the extent of observation and the depth of imaging is especially attractive. Thus, these microlenses can potentially be incorporated into accommodative contact lenses, endoscopes, laparoscopes, surveillance cameras, flexible displays, and many other miniaturized optical systems. Both reflective and transmissive FZPs could be beneficial to these applications. For instance, the reflective FZPs on a thin substrate could be used in contact lenses to produce images on the retina. The reflective types could be an alternative for costly deformable mirrors, which are used for focus scanning in microscopes. Miniaturized zoom lenses for small form-factor cameras (e.g. cell phones and surgical tools) is another potential application for reflective microlenses[33–35]. The Si-based fabrication technology for these FZP microlenses provides the potential for integration with electronic circuits on a single chip.

Methods

Fabrication process. The fabrication process starts with a P-type Si wafer with a thickness of 350 μm. A 100-nm-thick Al layer is deposited on the Si wafer to create a highly reflective surface. The Al layer is patterned with photolithography to create FZPs on the Si substrate. A 1-μm-thick layer of photoresist (PR) S-1813 (Shipley, Marlboro, MA, USA) is spun on the wafer. The PR is exposed to a 95 mJ/cm^2 dose of ultra-violet light and then immersed in a developer MF-391 (Shipley, Marlboro, MA, USA) to develop.

An Al etchant solution is used to etch Al for 3 min to create reflective zones on Si. Then, an inductively coupled plasma (ICP) etcher is used to form nanowires into the Si substrate to create dark zones. Sulfur hexafluoride (SF_6) and oxygen (O_2) are process gases in this etching step, where the temperature of the wafer chuck is maintained at −110 °C. The ICP power is set at 750 W, while the RIE power is 3 W. The etching time is 20 min. Sylgard 184 Silicone elastomer (Dow Corning, MI, USA) is spun on the wafer to create a 100-μm-thick PDMS layer. The wafer is placed in a vacuum chamber for 15 hr for the PDMS to degas and fill the voids between nanowires. The whole wafer is baked at 70 °C for 1 hr to improve the strength of the PDMS. Si on the backside of the wafer is removed with a dry, bulk etching process in the ICP etcher with SF_6 as the process gas. The ICP and RIE powers are 1500 W and 5 W, respectively, for this process. The chamber pressure is maintained at 15 mTorr.

Imaging setup. The imaging setup is modified from a commercial microscope, which consists of a wide-band light source, three lenses, a nonpolarized beam splitter and a camera. The object was placed in front of lens L_1 which is a 1-inch doublet lens with minimum chromatic aberration in the visible range. The light source with a filter is used to produce a narrow band (50 nm) light illumination with a central wavelength of 630 nm. A 20× Nikon objective lens L_2 with a numerical aperture (NA) of 0.4 and a working distance of 21 mm is used to illuminate the light onto the micro FZPs arrays. The high NA of lens L_2 allows for maximum collection of the reflected light from the micro FZPs. The NA of lens L_2 should be larger than the microlens array to maximize light interception. Aberrations of lenses should be small enough (less than 1-wave) to create sharp images. The overall focus of the system depends on the focal length and location of the lenses including micro FZPs and macro lenses. A digital CCD camera is used for imaging with high resolution (1920 × 1080 pixels). The diameter of the lens L_3 is 1 inch. The overall setup length is roughly 50 cm. Standard 1-inch diameter holders are used for mounting optical components.

References

1. Song, Y. M. *et al.* Digital cameras with designs inspired by arthropod eye. *Nature* **497,** 95–99 (2013).
2. Jeong, K.-H., Kim, J. & Lee, L. P. Biologically inspired artificial compound eyes. *Science* **312,** 557–561 (2006).
3. Floreano, D. *et al.* Miniature curved artificial compound eyes. *Proc. Natl. Acad. Sci. USA* **110,** 9267–9272 (2013).
4. Wu, D. *et al.* Bioinspired fabrication of high-quality 3D artificial compound eyes by voxel-modulation femtosecond laser writing for distortion-free wide-field-of-view imaging. *Adv. Opt. Mater.* **2,** 751–758 (2014).
5. Ko, H. C. *et al.* A hemispherical electronic eye camera based on compressible silicon optoelectronics. *Nature* **454,** 748–753 (2008).
6. Forrest, S. R. The path to ubiquitous and low-cost organic electronic appliances on plastic. *Nature* **428,** 911–918 (2004).
7. McAlpine, M. C., Friedman, R. S. & Lieber, C. M. High-performance nanowire electronics and photonics and nanoscale patterning on flexible plastic substrates. *Proc. IEEE* **93,** 1357–1363 (2005).
8. Discrete, J. S., Nomura, K., Ohta, H., Takagi, A. & Kamiya, T. Room-temperature fabrication of transparent flexible thin-film transistors using amorphous oxide semiconductors. *Nature* **432,** 488–492 (2004).
9. Eda, G., Fanchini, G. & Chhowalla, M. Large-area ultrathin films of reduced graphene oxide as a transparent and flexible electronic material. *Nat. Nanotechnol.* **3,** 270–274 (2008).
10. Gates, B. D. Flexible Electronics. *Science* **323,** 1566–1567 (2009).
11. Rajasekharan, R., Butt, H., Dai, Q., Wilkinson, T. D. & Amaratunga, G. A. J. Can nanotubes make a lens array? *Adv. Mater.* **24,** no. 23, 170–173 (2012).
12. Butt, H. *et al.* Cylindrical Fresnel lenses based on carbon nanotube forests. *Appl. Phys. Lett.* **101,** 243116 (2012).
13. Furlan, W. D., Saavedra, G. & Monsoriu, J. A. White-light imaging with fractal zone plates. *Opt. Lett.* **32,** 2109–2111 (2007).
14. Chu, Y. S. *et al.* Hard-x-ray microscopy with Fresnel zone plates reaches 40 nm Rayleigh resolution. *Appl. Phys. Lett.* **92,** 3–5 (2008).
15. Serre, D., Deba, P. & Koechlin, L. Fresnel Interferometric Imager: ground-based prototype. *Appl. Opt.* **48,** 2811 (2009).
16. Naulleau, P. P., Mochi, I. & Goldberg, K. A. Optical modeling of Fresnel zoneplate microscopes. *Appl. Opt.* **50,** 3678–3684 (2011).
17. Zhu, D., Li, C., Zeng, X. & Jiang, H. Tunable-focus microlens arrays on curved surfaces. *Appl. Phys. Lett.* **96,** 3–5 (2010).
18. Kim, Y. *et al.* Viewing-angle-enhanced integral imaging system using a curved lens array. *Opt. Express* **12,** 421–429 (2004).
19. Leem, J. W., Song, Y. M. & Yu, J. S. Biomimetic artificial Si compound eye surface structures with broadband and wide-angle antireflection properties for Si-based optoelectronic applications. *Nanoscale* **5,** 10455–10460 (2013).
20. Huang, C.-C. *et al.* Large-field-of-view wide-spectrum artificial reflecting superposition compound eyes. *Small* **10,** 3050–3057 (2014).
21. Duparré, J., Dannberg, P., Schreiber, P., Bräuer, A. & Tünnermann, A. Thin compound-eye camera. *Appl. Opt.* **44,** 2949–2956 (2005).
22. Tremblay, E. J., Stamenov, I., Beer, R. D., Arianpour, A. & Ford, J. E. Switchable telescopic contact lens. *Opt. Express* **21,** 15980–15986 (2013).
23. Anstice, N. S. & Phillips, J. R. Effect of dual-focus soft contact lens wear on axial myopia progression in children. *Ophthalmology* **118,** 1152–1161 (2011).
24. Flusberg, B. A. *et al.* Fiber-optic fluorescence imaging. *Nat. Methods* **2,** 941–950 (2005).
25. Fujimoto, J. G. Optical coherence tomography for ultrahigh resolution *in vivo* imaging. *Nat. Biotechnol.* **21,** 1361–1367 (2003).
26. Kanhere, A. *et al.* Multicamera laparoscopic imaging with tunable focusing capability. *J. Microelectromechanical Syst.* **23,** 1290–1299 (2014).
27. Zhu, R. *et al.* Polymeric-lens-embedded 2D/3D switchable displays with dramatically reduced crosstalk. *Appl. Opt.* **53,** 1388–1395 (2014).
28. Moghimi, M. J., Chattergoon, K. N., Wilson, C. R. & Dickensheets, D. L. High speed focus control MEMS mirror with controlled air damping for vital microscopy. *J. Microelectromechanical Syst.* **22,** 938–948 (2013).
29. Reddy, G. D., Kelleher, K., Fink, R. & Saggau, P. Three-dimensional random access multiphoton microscopy for functional imaging of neuronal activity. *Nat. Neurosci.* **11,** 713–720 (2008).
30. Pasteur, N., Philips, A., Fort, P. & Raymond, M. Flexible active-matrix electronic ink display. *Nature* **423,** 136 (2003).
31. Huang, Y.-F. *et al.* Improved broadband and quasi-omnidirectional anti-reflection properties with biomimetic silicon nanostructures. *Nat. Nanotechnol.* **2,** 770–774 (2007).

32. Hass, G. & Waylonis, J. E. Optical constants and reflectance and transmittance of evaporated aluminum in the visible and ultraviolet. *J. Opt. Soc. Am.* **51,** 719–722 (1961).
33. Kaylor, B. M. *et al.* Miniature non-mechanical zoom camera using deformable MOEMS mirrors. *SPIE Moems and Miniaturized Systems XI* **8252,** 3–9 (2012).
34. Jungwirth, M. E. L., Wick, D. V. & Dereniak, E. L. Theory and design of a MEMS-enabled diffraction limited adaptive optical zoom system. *SPIE Micro- and Nanotechnology Sensors, Systems, and Applications IV* 8373, 83730T (2012).
35. Lu, Y., Stockbridge, C. R., Hoffman, S. M. & Bifano, T. G. Variable zoom system with aberration correction capability. *J. Mod. Opt.* **59,** 1049–1055 (2012).

Acknowledgements

This project was supported by the National Institutes of Health (NIH) under Grant No. 1DP20D008678-01. This research utilized National Science Foundation (NSF) supported shared facility at the University of Wisconsin-Madison. The fabrication was partially carried out at Montana Microfabrication Facility (MMF) located at Montana State University-Bozeman. The authors would like to thank Dr. Yen-Sheng Lu, Professor David Dickensheets and his research group for their technical assistance, and Kari Van Grinsven for proofreading the manuscript.

Author Contributions

M.J.M. and H.J. conceived the idea and designed the device. H.J. supervised the research. M.J.M. fabricated the device. M.J.M., J.F. and A.K. tested the devices and captured images. M.J.M. and J.F. performed simulation. M.J.M. and H.J. wrote the manuscript. All authors read and revised the manuscript.

Additional Information

Supplementary information accompanies this paper at http://www.nature.com/srep

Competing financial interests: The authors declare no competing financial interests.

How to cite this article: Moghimi, M. J. *et al.* Micro-Fresnel-Zone-Plate Array on Flexible Substrate for Large Field-of-View and Focus Scanning. *Sci. Rep.* **5**, 15861; doi: 10.1038/srep15861 (2015).